Polymer 51 (2010) 5304–5308

Contents lists available at ScienceDirect

Polymer

journal homepage: www.elsevier.com/locate/polymer

Polymer Communication

Controlling the phase behavior of block copolymers via sequential block growth

Arif O. Gozen [a], Michelle K. Gaines [b,1], Mark W. Hamersky [c], Panagiotis Maniadis [d], Kim Ø. Rasmussen [d], Steven D. Smith [c], Richard J. Spontak [a,b,*]

[a] Department of Chemical and Biomolecular Engineering, North Carolina State University, Raleigh, NC 27695, USA
[b] Department of Materials Science and Engineering, North Carolina State University, Raleigh, NC 27695, USA
[c] Miami Valley Innovation Center, The Procter & Gamble Company, Cincinnati, OH 45061, USA
[d] Theoretical Division, Los Alamos National Laboratory, Los Alamos, NM 87545, USA

ARTICLE INFO

Article history:
Received 27 July 2010
Received in revised form
29 August 2010
Accepted 3 September 2010
Available online 15 September 2010

Keywords:
Block copolymer
Phase behavior
Mean-field theory

ABSTRACT

Block copolymers remain one of the most extensively investigated classes of polymers due to their abilities to self-organize into various nanostructures and modify polymer/polymer interfaces. Despite fundamental and technological interest in these materials, only a handful of experimental phase diagrams exist due to the laborious task of preparing such diagrams. In this work, two copolymer series are each synthesized from a single macromolecule via sequential living anionic polymerization to yield molecularly asymmetric diblock and triblock copolymers systematically varying in composition. The phase behavior and morphology of these copolymers are experimentally interrogated and quantitatively compared with predictions from mean-field theories, which probe copolymer phase behavior beyond current experimental conditions.

1. Introduction

Block copolymers, macromolecules composed of two or more chemically distinct species arranged in long, contiguous sequences that are covalently linked together, remain at the forefront of soft materials research due to their unique surfactant-like attributes [1,2]. Under favorable conditions, they can (*i*) self-organize into a wide variety of (a)periodic nanostructures and (*ii*) reduce interfacial tension along, and thus compatibilize, polymer/polymer interfaces. For these reasons, block copolymers are ubiquitous in a wide range of (nano)technologies that require multifunctionality and/or nanoscale structuring from an organic material [2–6]. The design of systems requiring the use of block copolymers necessarily demands an understanding of the phase behavior of these macromolecules, and numerous endeavors [7] have sought to provide theoretical frameworks by which to predict block copolymer phase behavior in the absence of scarce experimental phase diagrams [8–10]. Unlike conventional phase diagrams of polymer blends wherein two homopolymers are physically combined, block copolymer phase diagrams require synthesis of a new copolymer with specific block lengths for each composition. Block copolymer phase diagrams are often expressed in a mean-field format with the thermodynamic incompatibility (χN), where χ denotes the Flory–Huggins interaction parameter that scales as reciprocal temperature, and N is the number of repeat units along the copolymer backbone.

To help overcome the challenges of synthesizing different copolymers to explore, in experimental fashion, the phase behavior of block copolymers, we previously introduced [11] the idea of sequential living anionic polymerization to generate a series of copolymers systematically varying in composition from a single parent macromolecule. The initial objective of this approach was to discern the molecular conditions at which an AB diblock copolymer, which consists of two endblocks (or "tails") constrained by a single, shared junction, began to exhibit the phase and mechanical properties more commonly associated with those of an ABA triblock copolymer capable of forming a molecular network by means of midblock bridging [12]. Prior results demonstrated [11,13,14] that, when the second A endblock was sufficiently short, it remained mixed in the B matrix even after microphase separation of the (first) A and B blocks and furthermore served to reduce the interblock incompatibility. As the second A endblock was grown, however, it likewise microphase-separated from the B midblock and co-located with the first A endblock, thereby forcing the midblock to adopt a bridged or looped conformation (excluding the ill-favored formation of dangling ends [15]). To differentiate the two

* Corresponding author. Tel.: +1 919 417 3554; fax: +1 919 515 3465.
E-mail address: rich_spontak@ncsu.edu (R.J. Spontak).
[1] Present address: Electro-Optical Systems Laboratory, Georgia Tech Research Institute, Atlanta, GA 30332, USA.

0032-3861/$ – see front matter © 2010 Elsevier Ltd. All rights reserved.
doi:10.1016/j.polymer.2010.09.006

chemically identical endblocks, we referred to them as A_1 and A_2, where A_1 comprises the parent diblock copolymer and A_2 represents the progressively grown endblock. Additional examination of these copolymers also revealed [13] that, upon microphase separation of both endblocks, the A-rich microdomains contained bidisperse brushes if the lengths of the A_1 and A_2 endblocks differed.

In this work, we extend the utility of this synthetic strategy, schematically depicted in Fig. 1, to diblock copolymers and then compare experimental results obtained from both sequentially grown diblock and triblock copolymers to predictions from the mean-field theoretical framework developed by Mayes and Olvera de la Cruz [16]. A detailed analysis of the effect of block length on interblock mixing is presented, and theoretical predictions regarding phase behavior and nanostructural development beyond the current set of experimental conditions are discussed.

2. Experimental

In the AB diblock series, the parent homopolymer was polystyrene (PS) synthesized via living anionic polymerization in cyclohexane at 60 °C with *sec*-butyllithium as the initiator. According to size exclusion chromatography (SEC), its number-average molecular weight was 8.3 kDa. The parent material in the A_1BA_2 series was a poly(styrene-*b*-isoprene) diblock copolymer synthesized in the same fashion as above. The block masses were 9.4 (styrene) and 46 (isoprene) kDa, as discerned by SEC and proton nuclear magnetic resonance (^{1}H NMR) spectroscopy. In both cases, the molecular weights of the parent macromolecules were selected to ensure that the order–disorder transition temperature (T_{ODT}) could be measured without concern of degradation. Endblocks varying in length were grown as depicted in Fig. 1 by sequential living anionic polymerization under identical conditions, and the resultant copolymers were each subjected to SEC and ^{1}H NMR analyses. In all cases, polydispersities were 1.04 or less. Specimens for rheology, small-angle X-ray scattering (SAXS) and transmission electron microscopy (TEM) were prepared by compression molding a platen ≈1.2 mm thick of each copolymer. Discs measuring 30 mm in diameter were punched from each platen and heated to 170 °C under vacuum for 2 h, after which time the materials were cooled to ambient temperature.

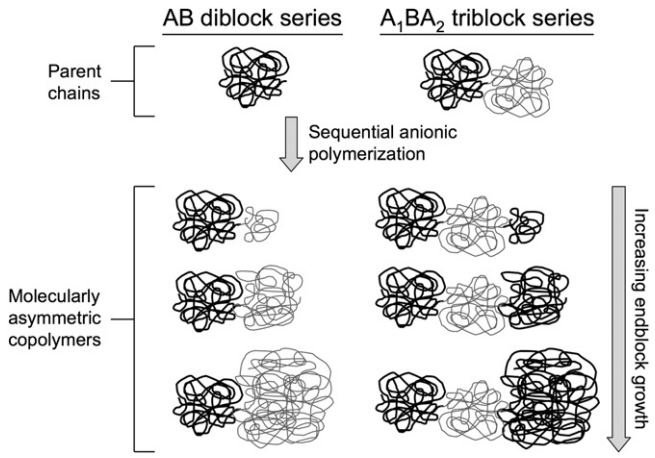

Fig. 1. Illustration of the sequential block growth strategy employed here, with the A and B blocks appearing black and gray, respectively. In the AB diblock series, PS serves as the parent chain onto which polyisoprene is grown, forming diblock copolymers differing in composition. In the A_1BA_2 triblock series, an A_1B diblock copolymer constitutes the parent macromolecule. Variation in the length of the A_2 block results in molecularly asymmetric triblock copolymers.

Dynamic shear measurements were conducted on an ARES rheometer equipped with 25 mm parallel plates separated by a 1 mm gap to measure T_{ODT} of each copolymer in both series. Details regarding the experimental procedure employed for this purpose were previously provided [11]. Briefly, measurements were conducted at low strain levels (2–5%) to ensure that linear viscoelasticity was maintained. Values of T_{ODT} were ascertained from abrupt reductions in the dynamic elastic (G') and viscous (G'') moduli during isochronal temperature sweeps performed at heating rates of 1 and 5 °C/min at a frequency of 1 rad/s. Specimens for TEM, obtained by cryoultramicrotomy at −100 °C, were selectively stained with the vapor of 2% OsO_4(aq) for 90 min and imaged on a Zeiss EM902 electron spectroscopic microscope, equipped with an in-column energy filter and operated at 80 kV. Two-dimensional SAXS patterns, acquired using CuKα radiation ($\lambda = 0.154$ nm) from a Rigaku RU-300 rotating anode operated at 40 kV and 40 mA, were azimuthally integrated to yield scattered intensity (I) as a function of wave vector (q), where $q = (4\pi/\lambda)\sin(\theta/2)$ and θ is the scattering angle.

3. Results and discussion

Values of T_{ODT} measured for each copolymer series are presented as a function of sequentially grown endblock (B in the AB series and A_2 in the A_1BA_2 series) mass in Fig. 2a and display two unexpected features. The first is that, in the A_1BA_2 series, a well-defined minimum is apparent when the A_2 block is relatively short. This observation has been attributed [11] to reduced incompatibility between the A_1 and B blocks due to short A_2 blocks remaining in the B matrix upon microphase separation of the A_1 and B blocks. Beyond a critical length (≈3.4 kDa), the A_2 blocks become

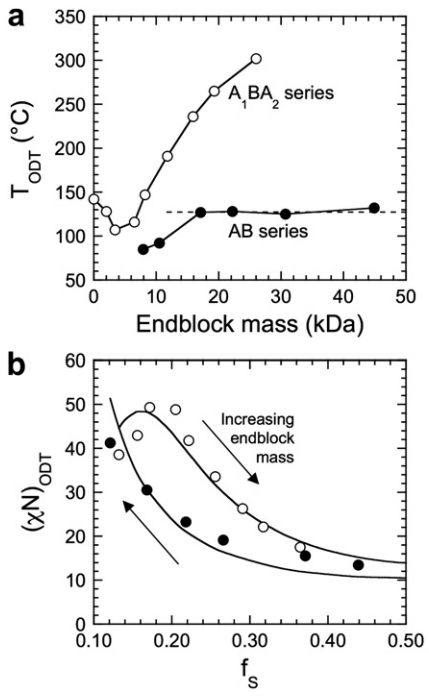

Fig. 2. Order–disorder transition (ODT) behavior of the AB diblock (●) and A_1BA_2 triblock (○) series generated in this study. Experimental ODT temperatures measured by rheology are presented in (a), and the solid lines connect the data. The dashed line corresponds to the average in the limit of large B blocks in the AB series. The mean-field representation showing $(\chi N)_{ODT}$ as a function of copolymer composition (f_S) is provided in (b), wherein the solid lines represent MFT predictions. Arrows identify the direction of increasing endblock growth in the two series.

sufficiently incompatible with the B matrix to likewise microphase-separate, co-locating with the A_1 blocks in A-rich microdomains. When this occurs, the B midblocks are forced to undergo conformational switching from tails anchored at just the A_1/B junction to either bridges or loops pinned down at both the A_1/B and A_2/B junctions [17,18]. Thus, the A_1BA_2 series under examination provides direct insight into the phase behavior of molecularly asymmetric triblock copolymers and, by inference, the condition signaling the onset of midblock bridging and network formation, as discussed elsewhere [13]. The second surprising feature evident in Fig. 2a is the plateau that develops in T_{ODT} when the B block in the AB series becomes sufficiently large, extending from 17 to 45 kDa. Over this range, T_{ODT} surprisingly appears to be nearly independent of the length of the sequentially grown B block ($=128 \pm 1.5$ °C), which implies that the shorter block in an AB diblock copolymer dictates the magnitude of T_{ODT}.

This latter observation appears contrary to previous theoretical predictions and conventional wisdom, which contend that an increase in molecular mass promotes an increase in thermodynamic incompatibility (i.e., χN). To determine if this is the case, the experimental data in Fig. 2a have been recast into a mean-field format in Fig. 2b. Doing so requires the temperature (T) dependence of χ, which is taken as $52.6/T - 0.0739$ from our previous analysis [11] of the triblock copolymer series and $33.0/T - 0.0228$ from a prior study of diblock copolymers by Lodge and co-workers [19]. Modest variations in these expressions may be due to differences in analysis or copolymer thermodynamics, and/or experimental error. The copolymer composition in Fig. 2b is expressed in terms of the number fraction of styrenic repeat units in the copolymer (f_S). The number of repeat units in block i is given by $M_i\rho_{r,i}/m_i$, where M_i is the mass of block i, m_i is the mass of repeat unit i, $\rho_{r,i}$ is the reduced mass density of repeat unit i given by the mass density of species i (1.04 and 0.913 g/cm^3 for polystyrene and polyisoprene, respectively) divided by the geometric-mean reference density. As the diblock copolymer series is sequentially grown, f_S decreases and $(\chi N)_{ODT}$ increases, confirming that an increase in chain length is accompanied by an increase in incompatibility, in favorable agreement with predictions from the mean-field theory (MFT) proposed by Mayes and Olvera de la Cruz [16] (included in Fig. 2b). While physical interpretation of the data in the triblock copolymer series is not so straightforward due to the mixing and conformational considerations discussed earlier, the corresponding MFT predictions accurately capture the shape and magnitude of the data, which suggests that this formalism can extend the current investigation to copolymers varying in composition and asymmetry.

Before doing so, however, morphological differences associated with changes in copolymer composition must be addressed. In the AB diblock series, f_S ranges from 44% (with the smallest B block) to 12% (with the largest B block), indicating that the copolymer series expectedly undergoes morphological transitions from lamellae to spherical micelles as the B block is grown. These transitions for diblock copolymers are well-established and are not reproduced here. The same is not true for the A_1BA_2 triblock series, which, despite the variation in f_S seen in Fig. 2b, remains isomorphic, retaining a hexagonally packed cylindrical morphology according to TEM and SAXS analyses over the entire series [13]. A representative TEM image acquired from the copolymer with $f_S = 0.36$ is displayed in Fig. 3a and confirms the existence of styrenic cylinders possessing limited long-range order in an isoprenic matrix. Images collected from copolymers with lower styrenic compositions likewise show evidence of a cylindrical morphology. Complementary results are obtained by SAXS patterns, an example of which is included in Fig. 3b. In this case (as well as others not shown here), the ratio of the second peak to the principal peak is $\sqrt{3}$, which is

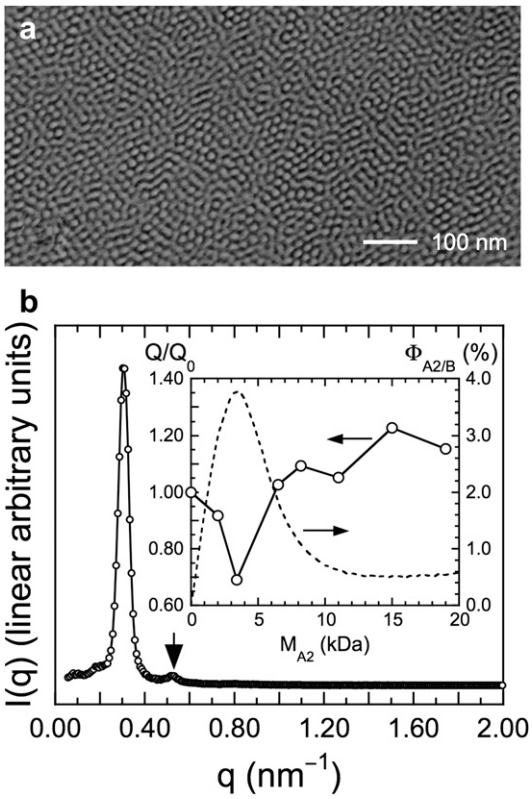

Fig. 3. Morphological characteristics of molecularly asymmetric A_1BA_2 triblock copolymers, as discerned by (a) TEM and (b) SAXS. The unsaturated midblocks of the copolymer (with a 19.3 kDa endblock) portrayed in (a) are selectively stained with the vapor of OsO_4(aq) and appear electron-opaque (dark) in this image. In the SAXS pattern (b), intensity is provided as a function of scattering vector (q) and displays a principal scattering peak and a discernible secondary peak (arrow). In the inset, the dependence of the normalized invariant (Q/Q_0) on endblock mass is provided. The solid lines serve to connect the data. Included in the inset are SCFT predictions for the fraction of the A_2 block residing in the B matrix ($\Phi_{A2/B}$, dashed line).

indicative of hexagonally packed cylinders. A third peak observed in the SAXS patterns of some copolymers further substantiates this morphological assignment. This result suggests that the phase boundaries delineating the morphologies of triblock copolymers can be shifted, thereby expanding or contracting regions of interest, by altering the extent of molecular asymmetry through sequential endblock growth.

A more detailed examination of Lorrentz-corrected SAXS patterns from the triblock series yields the scattering invariant (Q), which provides a measure of structural homogeneity and, thus, phase miscibility [20]. This quantity is determined from $1/2\pi i_e \int_0^\infty I(q)q^2dq$, where i_e denotes the Thompson scattering factor. For practical purposes, the integration is performed from the first datum point at low q to the value of q beyond which $I(q)$ does not change (1.5 nm^{-1}) [21]. Results from this analysis, normalized with respect to Q for the parent diblock (Q_0), are included in the inset of Fig. 3b and reveal the existence of a minimum (confirming improved phase miscibility) when the A_2 block is short, which coincides favorably with the minimum observed in T_{ODT} (*cf.* Fig. 2a). Included for comparison in the inset are predictions from self-consistent field theory (SCFT) for the fraction of A_2 residing in the core of the B matrix ($\Phi_{A2/B}$) as a function of A_2 block mass. Details of the SCFT framework and the numerical methods employed therein are provided elsewhere [22,23], and results from this theoretical approach have been previously shown [13] to accurately predict the morphological characteristics of microphase-ordered triblock copolymers varying in molecular asymmetry. It is important to note

that the minima measured in Q/Q_0 and T_{ODT} coincide embarrassingly well with the maximum in $\Phi_{A2/B}$ predicted by SCFT.

Verification of the applicability of the MFT and SCFT formalisms to the diblock and triblock copolymer systems under investigation in this work permits extension of these theories to molecularly asymmetric triblock copolymers varying in composition and symmetry beyond current experimental conditions. For convenience, we introduce τ as the molecular asymmetry factor, defined as the number of repeat units in the A_1 block relative to that in both the A_1 and A_2 blocks. Two particular values of τ warrant mention: (*i*) when $\tau = 1$, no A_2 block exists and the copolymer is a diblock; and (*ii*) when $\tau = 1/2$, the A_1 and A_2 blocks are identical, resulting in a molecularly symmetric triblock copolymer. Between $\tau = 1$ and $\tau = 1/2$, the A_2 blocks are shorter than the A_1 blocks, whereas values of τ less than 1/2 correspond to longer A_2 blocks. We also introduce β, the ratio of the number of B repeat units to that of A_1 repeat units, as a measure of the parent diblock copolymer composition. In the experimental measurements discussed earlier in this work, $\beta = 6.6$. With both τ and β as adjustable parameters, the lengths of the B and A_2 blocks can be independently varied. For simplicity, the length of the A_1 block is held constant, and only values of β greater than or equal to unity are considered further.

In Fig. 4a, values of $(\chi N)_{ODT}$ are presented as a function of τ for five different values of β. When $\beta = 1$ and the parent diblock copolymer is symmetric, addition of an A_2 block causes $(\chi N)_{ODT}$ to increase monotonically over the range of τ examined. This is not the case when $\beta = 2$, for which a weak maximum in $(\chi N)_{ODT}$ is apparent above $\tau = 1/2$, and a weak minimum appears below $\tau = 1/2$. As β (and, hence, the length of the B block) is increased, the maximum in $(\chi N)_{ODT}(\tau)$ shifts to lower values of τ and becomes more sharply pronounced. In contrast, the minimum observed below $\tau = 1/2$ when $\beta = 2$ disappears altogether. As in Fig. 2b and elsewhere for the case of $\beta = 2.6$, the maximum in $(\chi N)_{ODT}$ when τ lies between 1 and 1/2 translates into a minimum in T_{ODT} induced by mixing of relatively short A_2 blocks in the B matrix. The cases of $\beta = 1$ and $\beta = 2$, however, deviate from this trend, suggesting that the phase behavior of these triblock copolymer systems may differ, which is amenable to future experimental investigation. Predictions of $(\chi N)_{ODT}$ as a function of β for four values of τ are provided in Fig. 4b. The diblock and molecularly symmetric triblock cases (highlighted), as well as the intermediate case ($\tau = 0.7$), behave similarly, increasing for the most part with increasing β. The upturn in $(\chi N)_{ODT}$ at low β for the case of $\tau = 1/2$ becomes more pronounced when τ is decreased further to 0.2. Recall that, in this limit, the A_2 blocks are longer than the A_1 blocks and appear to have a more profound effect on copolymer phase behavior, especially when the B midblock is relatively short.

The MFT predictions displayed in Fig. 4 confirm that the constitution of the parent diblock, as well as the relative length of the sequentially grown A_2 block, can substantially influence the phase behavior, expressed in terms of the ODT, of molecularly asymmetric triblock copolymers. Complementary SCFT predictions reveal that, under isothermal conditions, both factors can likewise induce morphological conditions that depend sensitively on both τ and β. In most cases, a symmetry-induced transition from alternating lamellae to hexagonally packed cylinders or vice-versa (depending on the value of β) is predicted to occur, although the

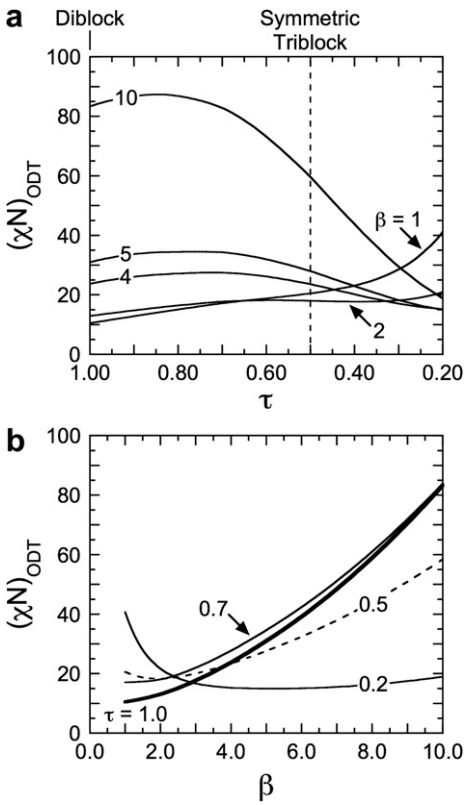

Fig. 4. Mean-field predictions of $(\chi N)_{ODT}$ for molecularly asymmetric A_1BA_2 triblock copolymers over a broad range of molecular characteristics, expressed in terms of asymmetry (τ, a) and parent diblock composition (β, b), as described in the text. In (a), $\tau = 1$ and $\tau = 1/2$ (dashed line) correspond to diblock and symmetric triblock copolymer designs (denoted), respectively, and values of β are labeled. In (b), the diblock and symmetric triblock cases are highlighted as bold and dashed lines, respectively, and values of τ are labeled.

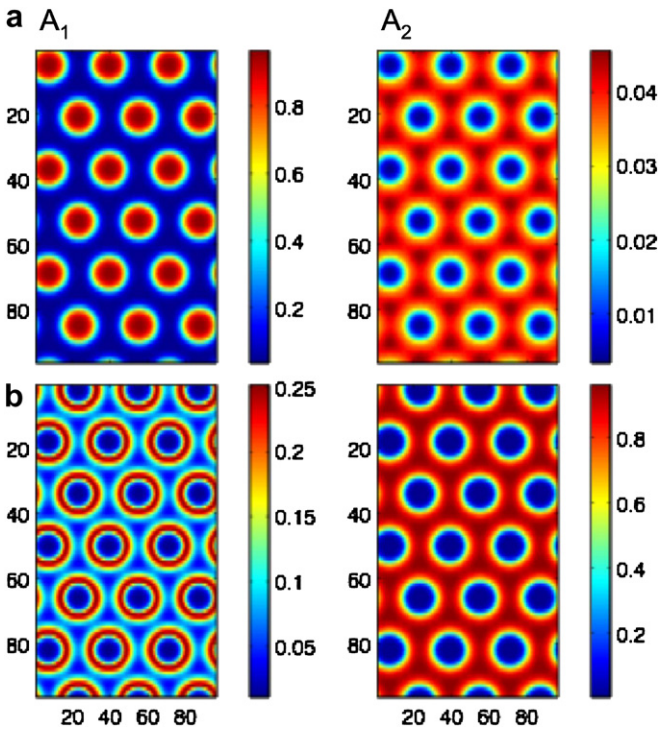

Fig. 5. Two-dimensional SCFT density profiles of the A_1 and A_2 blocks generated for the A_1BA_2 system in which $\beta = 2$ and τ is set equal to (a) 0.91 and (b) 0.16. In (a), the A_2 blocks are sufficiently short to remain mixed within the B-rich matrix that surrounds A_1-rich hexagonally packed cylinders. In (b), the A_2 blocks are longer than the A_1 blocks, and the system organizes into an inverted cylindrical morphology wherein the A_2 blocks comprise the matrix and the B blocks assemble into hexagonally packed cylinders. The shorter A_1 blocks co-reside with the A_2 blocks in the matrix, forming a corona around the cylinders.

bicontinuous gyroid morphology has been observed [24,25] in symmetric triblock copolymers. Of particular interest here is the system wherein $\beta = 2$, for which three different morphologies are observed as τ decreases. When $\tau = 0.91$, hexagonally packed cylinders of A_1 develop in a B matrix, as seen in the 2D density fields presented in Fig. 5a. In this panel, the short A_2 blocks remain primarily mixed within the B matrix, localizing at the interstitial region between A_1-rich cylinders. This scenario is similar to the one encountered in the present triblock series, and the SCFT predictions permit visualization of the block arrangements at thermodynamic equilibrium [22,23]. If τ is decreased to 0.5, the system organizes into a lamellar morphology in which the A_1 and A_2 blocks are indistinguishable, which is why we elect not to include those results here. In Fig. 5b, though, τ is decreased to 0.16 and the distributions of the A_1 and A_2 blocks are noticeably different. The longer A_2 blocks comprise the matrix, whereas the B midblocks assemble into hexagonally packed cylinders. The shorter A_1 blocks form a coronal shell around the B-rich cylinders so that the A-rich matrix becomes a bidisperse mixture of A_1 and A_2 endblocks. Thus, the SCFT results likewise indicate that the morphologies (as well as their stability ranges) of molecularly asymmetric triblock copolymers can be tuned by judicious choices of τ and β.

4. Conclusions

Families of diblock and triblock copolymers with sequentially grown endblocks provide an efficient means by which to explore, and ultimately exploit, the phase behavior of molecularly asymmetric block copolymers. In the diblock series investigated here, the ODT temperature is limited by the short, parent block when the sequential block becomes sufficiently large. In contrast, endblock mixing in the midblock-rich matrix of the copolymer morphology, independently confirmed from invariant analysis of scattering patterns, promotes an initial reduction in the ODT temperature in the triblock series. Such phase behavior is predicted by mean-field theory. Extension of this theory and self-consistent field theory to molecularly asymmetric triblock copolymers demonstrates a wealth of phase behavior that can be realized by systematically varying the composition of the parent diblock copolymer and the relative length of the sequentially grown endblock. In addition, these systems can be used to interrogate additional considerations, such as the conformation of the copolymer midblock, the critical endblock length required to induce microphase separation, and the role of bidisperse brushes on nanostructure-property development.

Acknowledgments

This work was supported, in part, by the Research Council of Norway under the NANOMAT Program and the Center for Integrated Nanotechnologies. M. K. G. expresses her gratitude for a GEM Fellowship and a NOBCChE Procter & Gamble Fellowship. Research at Los Alamos National Laboratory is carried out under the auspices of the National Nuclear Security Administration of the U.S. Department of Energy under Contract No. DE-AC52-06NA25396.

References

[1] Hamley IW. The physics of block copolymers. New York: Oxford University Press; 1998.
[2] Hadjichristidis N, Pispas S, Floudas G. Block copolymers – synthetic strategies, physical properties, and applications. Hoboken: John Wiley & Sons; 2003.
[3] Park C, Yoon J, Thomas EL. Polymer 2003;44:6725.
[4] Hamley IW. Angew Chem Int Ed 2003;42:1692.
[5] Lazzari M, Liu G, Lecommandoux S. Block copolymers in nanoscience. Weinheim: Wiley-VCH; 2007.
[6] Alemdaroğlu FE. DNA block copolymers – synthesis, morphologies, and applications: a combinatorial tool for cancer nanotechnology. Saarbrücken: VDM Verlag Dr. Müller Aktiengesellschaft & Co. KG; 2008.
[7] Matsen MW, Bates FS. Macromolecules 1996;29:1091.
[8] Khandpur AK, Förster S, Bates FS, Hamley IW, Ryan AJ, Bras W, et al. Macromolecules 1995;28:8796.
[9] Floudas G, Ulrich R, Wiesner U. J Chem Phys 1999;110:652.
[10] Bailey TS, Pham HD, Bates FS. Macromolecules 2001;34:6994.
[11] Hamersky MW, Smith SD, Gozen AO, Spontak RJ. Phys Rev Lett 2005;95:168306.
[12] See: Kane L, Norman DA, White SA, Matsen MW, Satkowski MM, et al Macromol Rapid Commun 2001;22:281. and the references cited therein.
[13] Smith SD, Hamersky MW, Bowman MK, Rasmussen KØ, Spontak RJ. Langmuir 2006;22:6465.
[14] Matsen MW. J Chem Phys 2000;113:5539.
[15] Nguyen-Misra M, Mattice WL. Macromolecules 1995;28:1444.
[16] Mayes AM, Olvera de la Cruz M. J Chem Phys 1989;91:7228.
[17] For a recent discussion of midblock bridging from an experimental standpoint, see: Takahashi Y Nihon Reoroji Gakkaishi 2009;37:211. and the references cited therein.
[18] For a recent discussion of physical gelation from a theoretical standpoint, see: Bras RE, Shull KR Macromolecules 2009;42:8513. and the references cited therein.
[19] Lodge TP, Pan C, Jin X, Liu Z, Zhao J, Maurer WW, et al. J Polym Sci B Polym Phys 1995;33:2289.
[20] Balta-Calleja F, Vonk C. X-ray scattering of synthetic polymers. London: Elsevier; 1989.
[21] Ryan AJ, Hamley IW, Bates FS. Macromolecules 1995;28:3860.
[22] Maniadis P, Thompson RB, Rasmussen KØ, Lookman T. Phys Rev E 2004; 69:031801.
[23] Maniadis P, Rasmussen KØ, Thompson RB, Kober EM. Int J Mol Sci 2009; 10:805.
[24] Laurer JH, Hajduk DA, Fung JC, Sedat JW, Smith SD, Gruner SM, et al. Macromolecules 1997;30:3938.
[25] Avgeropoulos A, Dair BJ, Hadjichristidis N, Thomas EL. Macromolecules 1997; 30:5634.